Available online at www.sciencedirect.com
SCIENCE DIRECT®
Journal of Solid State Chemistry 178 (2005) 3145–3151
JOURNAL OF SOLID STATE CHEMISTRY
www.elsevier.com/locate/jssc

Synthesis, structure and magnetic properties of the one-dimensional bimetallic oxide [Cu(terpy)Mo_2O_7]

Eric Burkholder[a], N. Gabriel Armatas[a], Vladimir Golub[b], Charles J. O'Connor[b], Jon Zubieta[a,*]

[a]*Department of Chemistry, Syracuse University, Syracuse, NY 13244, USA*
[b]*Advanced Materials Research Institute, University of New Orleans, New Orleans, LA 70148, USA*

Received 19 April 2005; received in revised form 22 July 2005; accepted 25 July 2005
Available online 25 August 2005

Abstract

The hydrothermal reaction of $Cu(CH_3CO_2)_2 \cdot H_2O$, Na_2MoO_4 and terpyridine at 140 °C for 48 h yields [Cu(terpy)Mo_2O_7] (**1**), a bimetallic one-dimensional oxide. The structure consists of ruffled chains of edge- and corner-sharing $\{MoO_5\}$ square pyramids, decorated with $\{CuN_3O_2\}$ '4 + 1' axially distorted square pyramids. The Cu(II) polyhedra are disposed so as to produce an alternating pattern of Cu–Cu distances across the $\{Mo_2O_2\}$ rhombi of the chain of 6.25 and 6.82 Å. This structural feature is reflected in the magnetic properties which are characteristic of a dimer rather than a linear chain, consistent with an alternating antiferromagnetic Heisenberg chain.

Keywords: Copper molybdate; Organic–inorganic hybrid material; One-dimensional bimetallic oxide; Alternating antiferromagnetic Heisenberg chain

1. Introduction

The contemporary interest in the rational design of new oxide materials reflects their vast compositional range, structural diversity, extensive physical properties and important applications [1–3]. In recent years, several strategies have been exploited in the design of new oxide materials. One attractive approach to synthetically modified inorganic oxides focuses on the structure-directing characteristics of organic molecules [4–7]. Incorporation of the organic species into the resultant organic–inorganic hybrid material combines the unique characteristics of the components to provide novel structural types, as well as new properties arising from the synergistic interplay of the two components [8].

In recent years, we have developed a synthetic strategy for the preparation of molybdenum and vanadium oxides which introduces the organic component as a ligand to a secondary metal cation [9–30]. This is a multicomponent system in which the organic subunit serves to fix a number of coordination sites about the secondary metal and to dictate the availability of attachment sites to the oxide substructure. Thus, the secondary metal-ligand coordination complex cation provides charge-compensation, as well as serving in space-filling, passivating and structure-directing roles. This general strategy has been most successful in the development of the chemistry of bimetallic oxides of the copper molybdate family Cu/Mo/O/ligand. Two distinct subgroups of this general family have been described: (i) a series consisting of polymeric molybdate substructures decorated by the secondary metal-ligand subunits [23–29] and (ii) structures constructed from discrete molybdate clusters bridged by the secondary metal-ligand component into chains, networks or frameworks [13–20,30].

As part of these investigations, the hydrothermal chemistry of Cu(II) with MoO_3 in the presence of

*Corresponding author. Fax: +1 315 443 4070.
E-mail address: jazubiet@syr.edu (J. Zubieta).

0022-4596/$ - see front matter © 2005 Elsevier Inc. All rights reserved.
doi:10.1016/j.jssc.2005.07.030

terpyridine was investigated. A novel one-dimensional copper molybdate [Cu(terpy)Mo_2O_7] (**1**) has been isolated. Curiously, the magnetic susceptibility studies of **1** indicates that this compound behaves as a Heisenberg spin dimmer or as an alternating antiferromagnetic Heisenberg chain.

2. Experimental section

2.1. General considerations

Reagents were purchased from Aldrich Chemicals and Lancaster Chemicals and used without further purification. Syntheses were carried out in 23 mL polytetrafluoroethylene-lined stainless steel containers under autogenous pressure. Water was distilled in house to a resistivity of ca. 3.0 M Ω using a Barstead model 525 Biopure distilled water center.

2.2. Synthesis of [Cu(terpy)Mo_2O_7] (1)

The reaction of Na_2MoO_4 (0.114, 0.554 mmol), $Cu(CH_3CO_2)_2 \cdot H_2O$ (0.044 g, 0.220 mmol), terpy (0.052 g, 0.223 mmol), As_2O_5 (0.069 g, 0.300 mmol), and H_2O (10.094 g, 560 mmol) in the mole ratio 2.5:0.98:1:1.3:2511 at 140 °C for 48 h provided aqua crystals of [{Cu(terpy)}Mo_2O_7] in 68% yield. Initial pH, 6.0; final pH, 6.0.

2.3. X-ray crystallography

Crystallographic data for the compound was collected with a Brüker P4 diffractometer equipped with a SMART CCD system [31] and using Mo-$K\alpha$ radiation ($\lambda = 0.71073$ Å). The data were collected at 90 K and corrected for Lorentz and polarization effects [32]. Absorption corrections were made using SADABS [33]. The structure solutions and refinements were carried out using the SHELXTL [34] crystallographic software package. The structure was solved using direct methods, and all of the nonhydrogen atoms were located from the initial solution. Crystal data for **1** are summarized in Table 1. Atomic positional coordinates and isotropic thermal parameters are given in Table 2, while selected bond lengths and angles for compound **1** are collected in Table 3. (CCDC reference no: CCDC 267890. See http://www.ccdc.cam.ac.uk for crystallographic data in CIF or other electronic format.)

2.4. Magnetism

The magnetic data were recorded on polycrystalline samples of **1** in the 2–300 K temperature range using a Quantum Design MPMS-5S SQUID spectrometer. Calibrating and operating procedures have been reported elsewhere [35]. The temperature-dependent magnetic data were obtained at a magnetic field of $H = 1000$ Oe.

Table 1
Summary of Crystallographic Data for [Cu(terpy)Mo_2O_7] (**1**)

Formula	$C_{15}N_3H_{11}CuMo_2O_7$
M	600.69
Crystal System	Triclinic
Space Group	$P\bar{1}$
a (Å)	8.7234(5)
b (Å)	10.2138(6)
c (Å)	11.0286(7)
α (deg)	91.949(1)
β (deg)	110.827(1)
γ (deg)	112.398(1)
V (Å^3)	832.65(9)
Z	2
D_{calc}, (g cm^{-3})	2.396
F (000)	582
μ (cm^{-1})	27.97
R_1, wR_2 [$I > 2\sigma(I)$][a]	0.0370, 0.0699
R_1, wR_2 [all data]	0.0447, 0.0722
$(\Delta\rho)_{max}$, $(\Delta\rho)_{min}$ (e Å^{-3})	0.919, −1.212
[a] $R_1 = \Sigma\|\|F_o\|-\|F_c\|\|/\Sigma\|F_o\|$, w$R_2 = [\Sigma w(F_O^2-F_c^2)^2/\Sigma w(F_o^2)^2]^{1/2}$	

Table 2
Atomic coordinates ($\times 10^4$) and equivalent isotropic displacement parameters (Å$^2 \times 10^3$) for [{Cu(terpy)}Mo_2O_7]. U_{eq} is defined as one third of the trace of the orthogonalized U_{ij} tensor

	x	y	z	U_{eq}
Mo(1)	4085(1)	3776(1)	3608(1)	6(1)
Mo(2)	5338(1)	817(1)	3872(1)	6(1)
Cu(1)	4157(1)	6975(1)	2997(1)	7(1)
O(1)	4816(3)	5761(2)	4190(2)	9(1)
O(2)	5610(3)	2830(2)	3997(2)	9(1)
O(3)	1969(3)	2720(3)	3522(2)	12(1)
O(4)	3749(3)	3874(3)	1977(2)	12(1)
O(5)	3655(3)	214(3)	2306(2)	12(1)
O(6)	4842(3)	−1068(2)	4377(2)	9(1)
O(7)	7368(3)	1162(3)	3784(2)	12(1)
N(1)	6483(4)	7880(3)	2710(3)	8(1)
N(2)	3224(4)	7350(3)	1231(3)	8(1)
N(3)	1462(4)	6160(3)	2607(3)	8(1)
C(1)	8167(5)	8226(4)	3606(3)	11(1)
C(2)	9676(5)	8930(4)	3326(4)	13(1)
C(3)	9451(5)	9248(4)	2084(4)	13(1)
C(4)	7716(5)	8887(4)	1148(4)	11(1)
C(5)	6258(4)	8242(3)	1503(3)	9(1)
C(6)	4377(4)	7941(3)	647(3)	8(1)
C(7)	3756(5)	8227(4)	−611(3)	9(1)
C(8)	1924(5)	7910(4)	−1240(3)	10(1)
C(9)	753(5)	7323(3)	−620(3)	9(1)
C(10)	1458(4)	7030(3)	629(3)	7(1)
C(11)	428(4)	6332(3)	1426(3)	7(1)
C(12)	−1428(4)	5871(3)	1012(3)	8(1)
C(13)	−2236(5)	5205(4)	1834(4)	12(1)
C(14)	−1190(5)	5012(4)	3035(3)	12(1)
C(15)	659(5)	5508(4)	3388(3)	11(1)

Table 3
Selected bond lengths (Å) and angles (deg) for [Cu(terpy)Mo2O7] (**1**)

Mo(1)–O(3)	1.712(2)	Mo(2)–O(2)	1.972(2)
Mo(1)–O(4)	1.729(2)	Mo(2)–O(6)#2	2.008(2)
Mo(1)–O(2)	1.868(2)	Cu(1)–O(1)	1.928(2)
Mo(1)–O(1)	1.888(2)	Cu(1)–N(2)	1.940(3)
Mo(1)–O(1)#1	2.228(2)	Cu(1)–N(1)	2.030(3)
Mo(2)–O(7)	1.708(2)	Cu(1)–N(3)	2.042(3)
Mo(2)–O(5)	1.719(2)	Cu(1)–O(6)#3	2.215(2)
Mo(2)–O(6)	1.953(2)		
O(3)–Mo(1)–O(4)	103.70(12)	O(2)–Mo(2)–O(6)#2	81.80(9)
O(3)–Mo(1)–O(2)	112.97(11)	O(1)–Cu(1)–N(2)	151.79(11)
O(4)–Mo(1)–O(2)	100.39(11)	O(1)–Cu(1)–N(1)	98.54(11)
O(3)–Mo(1)–O(1)	112.99(11)	N(2)–Cu(1)–N(1)	79.92(11)
O(4)–Mo(1)–O(1)	95.97(11)	O(1)–Cu(1)–N(3)	98.86(11)
O(2)–Mo(1)–O(1)	125.32(10)	N(2)–Cu(1)–N(3)	79.60(11)
O(3)–Mo(1)–O(1)#1	91.00(10)	N(1)–Cu(1)–N(3)	159.47(11)
O(4)–Mo(1)–O(1)#1	163.78(10)	O(1)–Cu(1)–O(6)#3	102.21(9)
O(2)–Mo(1)–O(1)#1	79.60(9)	N(2)–Cu(1)–O(6)#3	106.00(10)
O(1)–Mo(1)–O(1)#1	71.61(10)	N(1)–Cu(1)–O(6)#3	92.98(10)
O(7)–Mo(2)–O(5)	109.54(12)	N(3)–Cu(1)–O(6)#3	93.90(10)
O(7)–Mo(2)–O(6)	98.99(11)	Mo(1)–O(1)–Cu(1)	122.19(12)
O(5)–Mo(2)–O(6)	96.80(11)	Mo(1)–O(1)–Mo(1)#1	108.39(10)
O(7)–Mo(2)–O(2)	96.13(11)	Cu(1)–O(1)–Mo(1)#1	128.05(11)
O(5)–Mo(2)–O(2)	95.15(11)	Mo(1)–O(2)–Mo(2)	137.00(13)
O(6)–Mo(2)–O(2)	156.34(10)	Mo(2)–O(6)–Mo(2)#2	105.17(10)
O(7)–Mo(2)–O(6)#2	121.05(11)	Mo(2)–O(6)–Cu(1)#4	122.33(11)
O(5)–Mo(2)–O(6)#2	129.38(11)	Mo(2)#2–O(6)–Cu(1)#4	131.55(11)
O(6)–Mo(2)–O(6)#2	74.83(10)		

Symmetry transformations used to generate equivalent atoms: ♯1 $-x+1,-y+1,-z+1$; #2 $-x+1,-y,-z+1$; #3 $x, y+1,z$; #4 $x,y-1,z$

3. Results and discussion

Conventional hydrothermal techniques [36,37] have been demonstrated to be particularly effective for the preparation and crystallization of organic/inorganic hybrid materials, as the difficulties inherent in the different solubilities of the starting materials in aqueous media are minimized, while the synthesis temperatures do not effect decomposition of the organic components [38,39]. Thus, the reaction of $Cu(CH_3CO_2)_2 \cdot H_2O$, terpyridine, As_2O_5 and Na_2MoO_4 in water at 140 °C for 48 h provided **1** in good yield. Although the As_2O_5 starting material does not appear in the product, the reagent was required for crystal growth. The infrared spectrum of **1** exhibits a strong band at 921 cm^{-1} ascribed to ν(Mo═O) and a medium intensity feature at 790 cm^{-1} associated with ν(Mo–O–Mo).

As shown in Fig. 1, the structure of **1** consists of one-dimensional chains of edge- and corner-sharing $\{MoO_5\}$ and $\{CuN_3O_2\}$ square pyramids. The core of the structure is a zig-zag chain of $\{MoO_5\}$ axially distorted square pyramids. Within the chain, pairs of square pyramids form edge-sharing binuclear units with the apical oxo-groups of the two polyhedra adopting an *anti*-orientation with respect to the fused basal planes. Each molybdenum site of the binuclear unit engages in a corner-sharing interaction with an adjacent binuclear unit to produce the ruffled chain profile.

The Cu(II) '4 + 1' square pyramids nestle in the cavities formed by the folding of the molybdate chain and employ a basal and an apical site to bridge to two adjacent binuclear molybdate subunits through the oxo-groups defining the shared edge of the molybdate pairs. The remaining basal sites of the Cu(II) are occupied by the nitrogen donors of the terpy ligand.

Each Mo(VI) site exhibits two terminal oxo-groups, one doubly bridging oxo-group defining the corner sharing interaction between binuclear subunits (μ_2-OMo_2), and two triply bridging oxo-groups, linking two Mo sites and a Cu(II) site (μ_3-OMo_2Cu). The average molybdenum-terminal oxo-group distance of 1.717(2) Å is unexceptional, while the doubly bridging oxo-group exhibits unsymmetrical Mo–O bonds of 1.868(2) and 1.972(2) Å. The bonds within the Mo_2O_2 rhombus of the binuclear unit exhibit short-long alternation with Mo1–O1 of 1.888(2) and 2.228(2) Å and Mo2–O6 of 1.953(2) and 2.008(2) Å. The basal plane of the Cu(II) site is occupied by O1 at 1.928(2) Å, while the apical site, occupied by O6, is elongated at 2.215(2) Å. The Cu(II) square pyramids are disposed

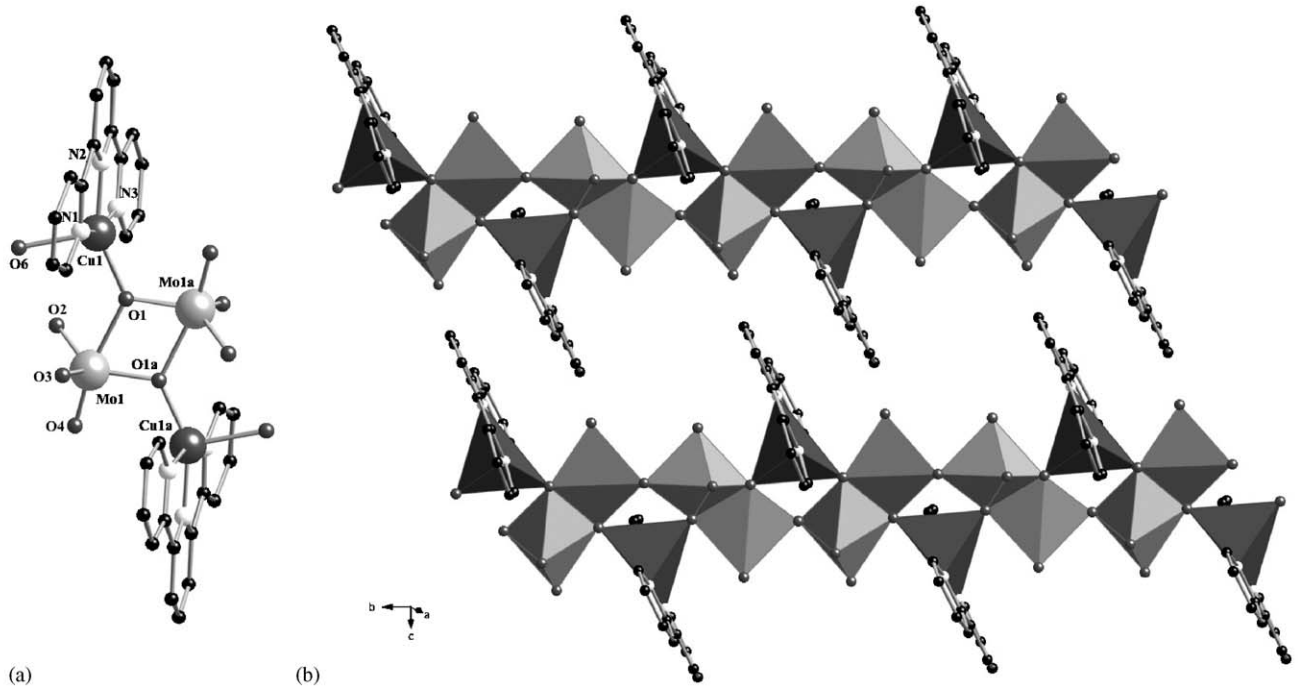

Fig. 1. (a) The atom-labeling scheme for [Cu(terpy)Mo_2O_7] (**1**). (b) A view of the one-dimensional structure of [Cu(terpy)Mo_2O_7] (**1**).

such that a given molybdate binuclear unit will share oxo-groups with two basal planes, while the adjacent binuclear unit shares oxo-groups with two apical sites. Consequently, the Cu–Cu distances across the $\{Mo_2O_2\}$ rhombi exhibit short-long alternation of 6.25 and 6.82 Å, respectively (Fig. 2).

One-dimensional molybdate structures are quite common and demonstrate considerable structural versatility, often reflecting the templating effects of the cationic components. The most common materials of this type consist of anionic molybdate chains and isolated charge-balancing cations, as represented by $[H_3NCH_2CH_2NH_3][Mo_3O_{10}]$ [40], $K_2[Mo_3O_{10}]$ [41], $(NH_4)_2[Mo_3O_{10}]$ [42], $Na(NH_4)[Mo_3O_{10}]$ [43], $[H_3N(CH_2)_6NH_3][Mo_4O_{13}]$ [43] and $[H_3N(CH_2)_2NH_2(CH_2)_2NH_3]_2$ $[Mo_9O_{30}]$ [44], as well as a number of dimolybdate systems, $\{Mo_2O_7\}_{\infty}^{2\infty-}$ [45–48]. Much less common are examples of neutral Mo_xO_y chains with organic ligands covalently attached to the molybdate sites, as in the materials of the $[(MoO_3)_n(2,2'\text{-bpy})_m]$ family [49]. Finally, there is a growing family of molybdate chains decorated with charge-balancing Cu(II)-ligand subunits [50–53]. It is noteworthy that, in common with **1**, four of the previously reported Cu/ligand/ molybdate chains are "dimolybdates": [Cu(2,2′-bpy)Mo_2O_7] [50], [Cu(pyrpyrz)Mo_2O_7] [51], [Cu(tpa)Mo_2O_7 [52], and [Cu(Me_2bpy)Mo_2O_7] [52] (pyrpyrz = 2,3-bis(2-pyridyl)pyrazine; tpa = tripyridylamine; Me_2bpy = 5,5′-dimethyl-2,2′-bispyridine). However, the structure of **1** is quite distinct from those previously reported, particularly with respect to the unusual alternation of Cu–Cu distances along the chain, a feature of some significance to the magnetic properties of **1**.

Organic/inorganic hybrid materials provide new opportunities in the realm of molecular magnetism for studying magnetically condensed systems [54,55]. In such materials, low-dimensional arrangements of the magnetic ions may be achieved through the use of nonmagnetic dividers such as fully oxidized metal ions or bulky organic substrates.

The magnetism of **1** may be attributed solely to the presence of Cu(II) ions ($3d^9$; $S = \frac{1}{2}$) which reside on the $\{CuMo_2O_7\}$ chains of the structure. Since Mo(VI) ($3d^0$; $S = 0$) ions do not possess an effective magnetic moment, they do not contribute to the bulk properties. Furthermore, the bimetallic oxide chains are insulated from one another by the bulky terpy ligands which project into the interchain domains. As a result Cu–Cu distances between chains are greater than 8.45 Å, precluding significant interchain interactions. Consequently, the magnetic properties of **1** may be described by models for low-dimensional cooperative phenomena.

The temperature dependence of the magnetic susceptibility of **1** is shown in Fig. 3. The effective moment of the compound (μ_{eff}) decreases as the

$$\mu_{eff} = \sqrt{8(\chi - \chi_{TI})T}, \quad (1)$$

where χ_{TI} is a temperature-independent contribution to the magnetic susceptibility.

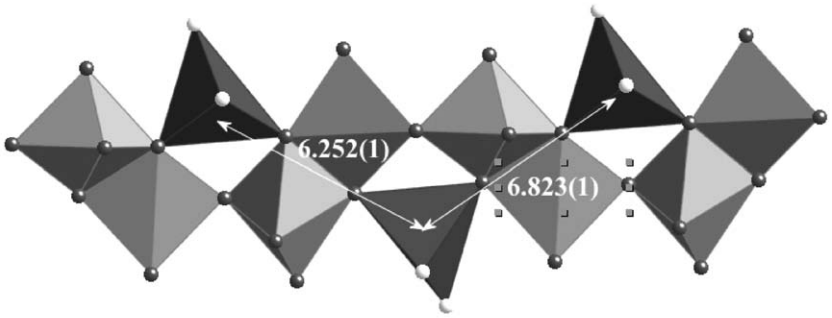

Fig. 2. The distinct Cu–Cu interactions across the $\{Mo_2O_2\}$ rhombi of the chain.

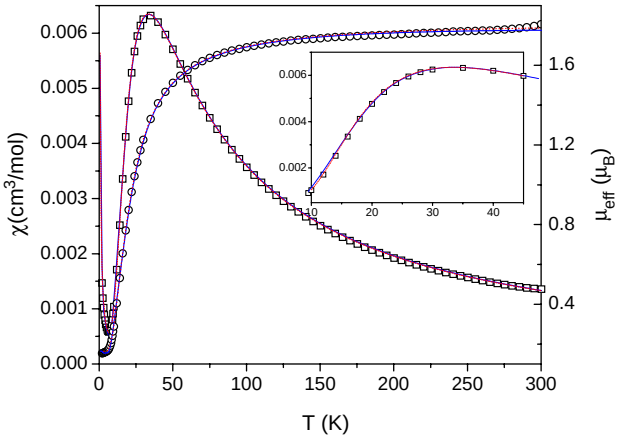

Fig. 3. The dependence of the magnetic susceptibility χ(□) and effective magnetic moment μ_{eff} (○) of **1** on temperature T. The lines drawn through the data are the fits to the Heisenberg dimer model (red dot line) and Heisenberg alternating chain model (solid blue line). The insert shows the comparison of the low-temperature fit for the Heisenberg dimer model and the Heisenberg alternating chain model.

temperature decreases, consistent with the presence of an intrachain antiferromagnetic interaction. However, the magnetic data could not be fit to the simple Heisenberg linear chain model with reasonable parameters. The behavior of the magnetic susceptibility is characteristic of a dimer rather than of a simple linear chain, reminiscent of a spin-Peierls distorted system. [56,57]

Consequently, the data were first fit to the Heisenberg dimer model with $S = \frac{1}{2}$ for the d^9 Cu(II) site taking into consideration the presence of monomeric paramagnetic impurities with the concentration x:

$$\chi = (1-x)\frac{N_A g^2 \mu_B^2}{k_B T}\frac{2\exp(2J/k_B T)}{1+3\exp(2J/k_B T)} + x\frac{N_A g^2 \mu_B^2}{2k_B T} + \chi_{TI}, \quad (2)$$

where x is the concentration of monomeric paramagnetic impurities, N_A = Avogadro's constant, k_B is the Boltzman constant, μ_B is the Bohr magnetism, J and αJ are the exchange integrals between a spin and its right and left neighbors, respectively, and H is the magnetic field.

The best fit for the calculated susceptibility χ_0 gave $g = 2.13$, $J = -27.1\,K$, $\chi_{TI} = -0.00003\,cm^3/mol$, and $x = 0.001$.

The data were then fit to an alternating antiferromagnetic Heisenberg chain model

$$H = -2J\sum_{i=1}^{n/2}[\hat{S}_{2i}\cdot\hat{S}_{2i-1} + \alpha\hat{S}_{2i}\cdot\hat{S}_{2i+1}] \quad (3)$$

using the extrapolation formula (4) [58]:

$$\chi = \frac{N_A g^2 \mu_B^2}{k_B T}\frac{A + By + Cy^2}{1 + Dy + Ey^2 + Fy^3}, \quad (4)$$

where $y = |J|/k_B T$. The values for parameters A, B, C, D, E and F for $0 \leqslant \alpha \leqslant 0.4$ were:

$A = 0.25$, $B = -0.12587 + 0.22752\alpha$, $C = 0.019111 - 0.13307\alpha + 0.509\alpha^2 - 1.3167\alpha^3 + 1.0081\alpha^4$, $D = 0.10772 + 1.4192\alpha$, $E = -0.0028521 - 0.42346\alpha + 2.1953\alpha^2 - 0.82412\alpha^3$, $F = 0.37754 - 0.067022\alpha + 5.9805\alpha^2 - 2.1678\alpha^3 + 15.838\alpha^4$. The values for parameters A–F for $0.4 < \alpha \leqslant 1$ were: $A = 0.25$, $B = -0.13695 + 0.26387\alpha$, $C = 0.017025 - 0.12668\alpha + 0.49113\alpha^2 - 1.1977\alpha^3 + 0.87257\alpha^4$, $D = 0.070509 + 1.3042\alpha$, $E = -0.0035767 - 0.40837\alpha + 3.4862\alpha^2 - 0.73888\alpha^3$, $F = 0.36184 - 0.065528\alpha + 6.65875\alpha^2 - 20.945\alpha^3$. The calculated susceptibility was corrected for the presence of monomeric paramagnetic impurities with the concentration x and the temperature-independent component TI. The best fit was $g = 2.17(1)$, $J = -26.5(3)\,K$, $\alpha = 0.170(4)$, $\chi_{TI} = -0.00003(1)\,cm^3/mol$, and $x = 0.0010(1)$. The value obtained for the g-factor was consistent with the value derived from the EPR spectrum (2.15–2.16) at room temperature. The value of μ_{eff} at 300 K per Cu(II) ion is $1.78\,\mu_B$. These results are similar to those previously reported for [Cu(II)(H_2O){(N-salicylaldiminato)glycinate}] [57].

4. Conclusion

The one-dimensional bimetallic oxide [Cu(terpy)-Mo_2O_7] (**1**) was prepared by hydrothermal methods. The structure consists of folded $\{Mo_2O_7\}_{\infty}^{2\infty-}$ chains of corner- and edge-sharing Mo(VI) octahedra, decorated with $\{Cu(terpy)\}^{2+}$ subunits. The Cu(II) '4+1' square pyramids are disposed along the chain so as to exhibit alternating Cu–Cu distances of 6.25 and 6.82 Å across the $\{Mo_2O_2\}$ rhombi of the chain. This structural feature is reflected in the magnetism which is consistent with an alternating antiferromagnetic Heisenberg chain rather than a simple linear chain.

5. Supplementary materials

Additional material available from the Cambridge Crystallographic Data Centre, CCDC no. 267890, comprises the final atomic coordinates for all atoms, thermal parameters, and a complete listing of bond distances and angles. Copies of this information may be obtained free of charge on application to The Director, 12 Union Road, Cambridge, CB2 2EZ, UK (fax +44-1223-336033; email: data_request@ccdc.cam.ac.uk or http://www.ccdc.cam.ac.uk).

Acknowledgments

This work was supported by a grant from the National Science Foundation, CHE-0242153 and by the Defense Advanced Research Projects Agency (MDA972-04-1-0029).

References

[1] W.H. McCarroll, in: R.B. King, (Ed.), Encyclopedia of Inorganic Compounds, vol. 6, Wiley, New York, 1994, pp. 2903–2946.
[2] G.K. Cheetham, Science 264 (1994) 794.
[3] D.W. Bruce, D. O'Hare, Wiley, Chichester, 1992.
[4] C.R. Kagan, D.B. Mitzi, C.D. Dimitrakopoulos, Science 286 (1999) 945.
[5] (a) D.B. Mitzi, J. Chem. Soc. Dalton Trans. 1 (2001);
(b) D.B. Mitzi, Inorg. Chem. 39 (2000) 6107.
[6] (a) S.I. Stupp, P.V. Braun, Science 27 (1997) 1242;
(b) M.E. Davis, A. Katz, W.R. Ahmad, Chem. Mater. 8 (1996) 1820.
[7] P.J. Hagrman, D. Hagrman, J. Zubieta, Angew. Chem. Int. Ed. Engl. 38 (1999) 2639.
[8] (a) J. Portier, J.-H. Choy, M.A. Subramamian, Int. J. Inorg. Mater. 3 (2001) 581;
(b) C. Sanchez, G.J. de A.A. Soler-Illia,, F. Ribot, T. Lalot, C.R. Mayer, V. Calwil, Chem. Mater. 13 (2001) 3061 and references therein
(c) C. Sanchez, F. Ribot, eds., Proceedings of the First European Workshop of Hybrid Organic–Inorganic Materials. Special issue of New J. Chem. 18 (1994);
(d) M.E. Davis, W.B. Lin, J. Am. Chem. Soc. 123 (2001) 10395;
(e) H. Li, M. Eddaoudi, M. O'Keeffe, O.M. Yaghi, Nature 402 (1999) 276;
(f) C.F. Blanford, T.N. Do, B.T. Holland, A. Stein, Mater. Res. Soc. Symp. Proc. 549 (1999) 61;
(g) L. Carlucci, G. Ciani, M. Moret, D.M. Proserpio, S. Rizzato, Angew. Chem. Int. Ed. 39 (2000) 1506;
(h) J.A. Swift, M.D. Ward, Chem. Mater. 12 (2000) 1501;
(i) H.K. Chae, M. Eddaoudi, J. Kim, S.I. Hauck, J.F. Hartwig, M. O'Keeffe, O.M. Yaghi, J. Am. Chem. Soc. 123 (2001) 11,482;
(j) H.R. Zhao, A. Heintz, X. Ouyang, K.R. Dunbar, C.F. Campana, R.D. Rogers, Chem. Mater. 11 (1999) 736.
[9] Y. Zhang, J.R.D. DeBord, C.J. O'Connor, R.C. Haushalter, A. Clearfield, J. Zubieta, Angew. Chem. Int. Ed. Engl. 35 (1996) 989.
[10] R.L. LaDuca Jr., R.C. Finn, J. Zubieta, Chem. Commun. (1999) 1669.
[11] R.L. LaDuca Jr., R.S. Rarig Jr., J. Zubieta, Inorg. Chem. 40 (2001) 607.
[12] P.J. Hagrman, C. Bridges, J.E. Greedan, J. Zubieta, J. Chem. Soc. Dalton Trans. (1999) 2901.
[13] P.J. Hagrman, D. Hagrman, J. Zubieta, Angew. Chem. Int. Ed. Engl. 38 (1999) 2638.
[14] D. Hagrman, C. Zubieta, R.C. Haushalter, J. Zubieta, Angew. Chem. Int. Ed. Engl. 36 (1997) 873.
[15] D. Hagrman, C. Sangregorio, C.J. O'Connor, J. Zubieta, J. Chem. Soc. Dalton Trans. (1998) 3707.
[16] D. Hagrman, P. Hagrman, J. Zubieta, Inorg. Chim. Acta 300–302 (2000) 212.
[17] J.R.D. DeBord, R.C. Haushalter, L.M. Meyer, D.J. Rose, P.J. Zapf, J. Zubieta, Inorg. Chim. Acta 256 (1997) 165.
[18] D. Hagrman, P.J. Zapf, J. Zubieta, Chem. Commun. (1998) 1283.
[19] D. Hagrman, P.J. Hagrman, J. Zubieta, Angew. Chem. Int. Ed. Engl. 38 (1999) 3165.
[20] D. Hagrman, J. Zubieta, C.R. Acad. Sci. Ser. Iic 3 (2000) 231.
[21] D. Hagrman, P.J. Hagrman, J. Zubieta, Comments Inorg. Chem. 21 (1999) 225 and references therein.
[22] D.J. Chesnut, D. Hagrman, P.J. Zapf, R.P. Hammond, R. LaDuca Jr., R.C. Haushalter, J. Zubieta, Coord. Chem. Rev. 190–192 (1999) 737.
[23] P.J. Zapf, R.P. Hammond, R.C. Haushalter, J. Zubieta, Chem. Mater. 10 (1998) 1366.
[24] D. Hagrman, C.J. Warren, R.C. Haushalter, C. Seip, C.J. O'Connor, R.S. Rarig Jr., K.M. Johnson III, R.L. LaDuca Jr., J. Zubieta, Chem. Mater. 10 (1998) 3294.
[25] D. Hagrman, R.C. Haushalter, J. Zubieta, Chem. Mater. 10 (1998) 361.
[26] M.C. Laskowski, R.L. LaDuca Jr., R.S. Rarig Jr. J. Zubieta, J. Chem. Soc. Dalton Trans. (1999) 3467.
[27] D.E. Hagrman, J. Zubieta, J. Solid State Chem. 152 (2000) 141.
[28] R.L. LaDuca Jr., M. Desciak, M. Laskowski, R.S. Rarig Jr., J. Zubieta, J. Chem. Soc. Dalton Trans. (2000) 2255.
[29] P.J. Zapf, C.J. Warren, R.C. Haushalter, J. Zubieta, Chem. Commun. (1997) 1543.
[30] D.G. Allis, R.S. Rarig, E. Burkholder, J. Zubieta, J. Mol. Struct. 688 (2004) 11.
[31] SMART, Data Collection Software, version 4.050, Siemens Analytical Instruments Inc., Madison, WI, 1996.
[32] SAINT, Data Reduction Software, version 4.050, Siemens Analytical Instruments Inc., Madison, WI, 1996.
[33] G.M. Sheldrick, SADABS, University of Göttingen, 1996.
[34] SHELXTL PC, Siemens Analytical X-ray Instruments Inc., Madison, WI, 1993.
[35] C.J. O'Connor, Prog. Inorg. Chem. 29 (1979) 203.
[36] M.S. Whittingham, Curr. Opin. Solid Sate Mater. Sci. 1 (1996) 227.
[37] J. Gopalakrishnan, Chem. Mater. 7 (1995) 1265.

[38] J. Zubieta, Comprehensive Coord. Chem. II 1 (2004) 697.
[39] D. Hagrman, P.J. Hagrman, J. Zubieta, Comments Inorg. Chem. 21 (1999) 225.
[40] M.I. Khan, Q. Chen, J. Zubieta, Inorg. Chim. Acta 213 (1993) 325.
[41] B.M. Gatehouse, P. Leverett, J. Chem. Soc. A (1968) 1398.
[42] K. Range, A. Fassler, Acta Crystallogr. Sect. C (46) (1990) 488.
[43] Y. Xu, L.-H. An, L.-L. Koh, Chem. Mater. 8 (1996) 814.
[44] L. Xu, C. Qin, X. Wang, E. Wang, Y. Wei, Inorg. Chem. 42 (2003) 7342.
[45] A.W. Armour, M.G.H. Drew, P.C.H. Mitchell, J. Chem. Soc. Dalton Trans. (1975) 1493.
[46] M. Seleborg, Acta Chem. Scand. 21 (1967) 499.
[47] H.-U. Hrausler, A. Förster, J. Fuchs, Z. Naturforsch B 35 (1980) 242.
[48] S.A. Hodorowicz, W. Lasocha, Cryst. Res. Technol. 23 (1988) K43.
[49] P.J. Zapf, R.C. Haushalter, J. Zubieta, Chem. Mater. 9 (1997) 2019.
[50] P.J. Zapf, C.J. Warren, R.C. Haushalter, J. Zubieta, Chem. Commun. (1997) 1543.
[51] R.S. Rarig Jr., P.J. Hagrman, J. Zubieta, Solid State Sci. 4 (2002) 77.
[52] R.S. Rarig, C. Bewley, E. Burkholder, J. Zubieta, Indian J. Chem. 42A (2003) 2235.
[53] Z. Kong, L. Weng, D. Tan, H. He, B. Zhang, J. Kong, B. Yue, Inorg. Chem. 43 (2004) 5676.
[54] C. Hornick, P. Rabu, M. Dillon, Polyhedron 19 (2000) 259.
[55] R.S. Rarig Jr., R. Lam, P.Y. Zavalij, J.K. Ngala, R.L. LaDuca, J.E. Greedan, J. Zubieta, Inorg. Chem. 41 (2002) 2124.
[56] R.E. Peierls, Quantum Theory of Solids, Oxford, 1955.
[57] W.E. Hatfield, L.W. ter Haar, Ann. Rev. Mater. Sci. 12 (1982) 177.
[58] W.E. Hatfield, J. Appl. Phys. 52 (1981) 1985.